

LIQUID CIRCULATION IN A CYLINDRICAL VESSEL WITH RADIAL BAFFLES AND INCLINED BLADE IMPELLER*

Ivan FOŘT^a, Miloslav HOŠŤÁLEK^b and Jaroslav MEDEK^c

^a Department of Chemical and Food Process Equipment Design, Czech Technical University, 166 07 Prague 6

^b Chemopetrol — Research Institute of Inorganic Chemistry, 400 60 Ústí nad Labem and

^c Department of Chemical and Food Process Equipment Design, Technical University, 619 69 Brno

Received June 1, 1988

Accepted September 7, 1988

Liquid circulation was studied in a cylindrical vessel with radial baffles under the turbulent flow regime of liquid agitated gradually with the following types of four inclined blade impellers: impeller with plane blades inclined at the angle of 25°; impeller with asymmetrically profiled blades at the angle of 30°—17°; impeller with strength-profiled blades. By solving the turbulent (vortex) analogy of the Stokes equations for the creeping (non-inertial) laminar flow, the streamline distribution (the Stokes stream function) in the bulk of agitated charge was obtained for each of impellers studied (relative size $d/D = 1/3$, relative distance from the bottom $H_2/D = 1/3$, relative vessel filling $H/D = 1$), placed axisymmetrically in the vessel and pumping the liquid towards its flat bottom. The zero values of the Stokes stream function at the bottom, walls, and charge liquid level, and further the radial profiles of axial and radial component of mean velocity in the cross sections under and above the impeller obtained experimentally by the laser-doppler anemometry on the assumption of axial symmetry of the agitated system studied were set as the boundary conditions for the solution of the partial differential equation considered. It follows from the results obtained that the homogenous circulation of agitated charge at the relatively lowest value of the impeller power input is reached when agitating with the asymmetrically profiled blade impeller which therefore can successfully replace the propeller mixer with airfoil profiled blades.

The inclined blade impellers are used in chemical and food industry above all for the homogenization of liquids, suspending of solid particles in liquids, and intensification of heat transfer between the jacketed vessel wall and agitated charge. These rotary high-speed impellers utilize the supplied power input above all to bring about the intensive circulation of agitated charge, and therefore we can see the effort of designers of these types of impellers to design such types of their blades which are well round streamed, and the impeller power input is then dissipated mostly in the bulk phase of agitated charge^{1,2}. The aim of this work is to compare the charge

* Part LXXVI in the series Studies on Mixing; Part LXXV Collect. Czech. Chem. Commun. 54, 633 (1989).

circulation agitated with three types of inclined blade impellers, and to recommend such a type which would cause the homogeneous circulation of charge with the lowest power input under the turbulent regime of flow.

THEORETICAL

Let us consider an agitated system (see Fig. 1) formed by a flat bottomed cylindrical vessel equipped with radial baffles at its wall. An inclined blade impeller rotates in the vessel axis in such a direction to pump liquid towards bottom. A cylindrical coordinate system is introduced in the system with the origin of coordinates at the point of intersection of the vessel axis of symmetry and its bottom. The three-dimensional velocity field is described by three velocity components: axial— w_{ax} , radial— w_{rad} , and tangential— w_{ϕ} . The following simplifying assumptions are assumed to be fulfilled in the system considered:

1) The charge is a homogeneous Newtonian liquid. 2) The process considered is isothermal and quasistationary. 3) The time-averaged flow is axisymmetric. 4) The turbulent flow may be considered fully developed. 5) The mass and momentum transport takes place mostly by eddy diffusion. 6) The shape of liquid level is not influenced by the charge motion (flow). 7) The effect of dimensions of laminar sub-layer at the walls, bottom, and baffles may be neglected.

The solution of the flow equation for our case is analogous to the Stokes simplification of the motion equation for the creeping laminar model described and verified for the turbulent flow of agitated charge in preceding parts of this series³⁻⁶.

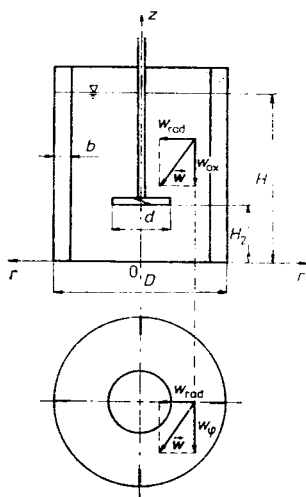


FIG. 1

Sketch of agitated system; $d/D = 1/3$, $H/D = 1$, $H_2/d = 1$, $b/D = 1/10$, $D = 0.297$ m

In our case we can write

$$E^2(E^2\bar{\psi}^2) = 0, \quad (1)$$

where the differential operator E^2 takes in cylindrical coordinates the form

$$E^2 = \frac{\partial^2}{\partial r^2} - \frac{1}{r} \frac{\partial}{\partial r} + \frac{\partial^2}{\partial z^2}, \quad (2)$$

the stream function is for mean flow defined by the relations

$$\bar{w}_{\text{rad}} = \frac{1}{r} \frac{\partial \bar{\psi}}{\partial z}, \quad \bar{w}_{\text{ax}} = -\frac{1}{r} \frac{\partial \bar{\psi}}{\partial r}, \quad (3a, b)$$

and the vorticity with respect to the assumptions introduced by the relations

$$\bar{\Omega}_\varphi = \frac{1}{r} E^2 \bar{\psi}, \quad \bar{\Omega}_{\text{ax}} = \bar{\Omega}_{\text{rad}} = 0. \quad (4a, b)$$

The solution of Eq. (1) can be found by the method of separation and variation of constants in the form of infinite series³

$$\bar{\psi} = r \sum_{i=1}^{\infty} J_1(k_i r) P(k_i z), \quad (5)$$

when on using definition relations (3) and (4), we obtain, for the corresponding non-zero components of mean velocity and vorticity, the relations

$$\bar{w}_{\text{rad}} = \sum_{i=1}^{\infty} J_1(k_i r) P'(k_i z), \quad (6a)$$

$$\bar{w}_{\text{ax}} = -\sum_{i=1}^{\infty} J_0(k_i r) k_i P(k_i z), \quad (6b)$$

or

$$\bar{\Omega}_\varphi = \sum_{i=1}^{\infty} J_1(k_i r) [P''(k_i z) - k_i^2 P(k_i z)]. \quad (7)$$

Here J_0 and J_1 is the Bessel cylindrical function of the first kind of index 0 or 1, respectively, and P the hyperbolic function of the form⁵

$$\begin{aligned} P(k_i z) = & B_i \cosh(k_i z) + C_i \sinh(k_i z) + \\ & + D_i \{k_i(z - z_0) \sinh(k_i z) - \sinh[k_i(z - z_0)] \sinh(k_i z_0)\} + \\ & + E_i \{k_i(z - z_0) \cosh(k_i z) - \sinh[k_i(z - z_0)] \cosh(k_i z_0)\}. \end{aligned} \quad (8)$$

The characteristic numbers of the problem k_i are given⁶ by

$$k_i = 2\lambda_i/D, \quad i = 1, 2, \dots, \quad (9)$$

where D is the vessel diameter and λ_i is the i -th root of transcendental function J_1 . The system is divided into three regions: 1, 2, and 3 – see Fig. 2. Integration constants B_i , C_i , D_i , and E_i are found for each of the regions described from boundary conditions on their lower ($z = z_0$) and upper base ($z = z_1$), respectively. As a matter of fact, on the vessel bottom (lower base of region 1) and on the liquid level of charge (upper base of region 3), function P must fulfil the conditions⁴

$$P(k_i z) = 0, \quad i = 1, 2, \dots, \quad z = 0, H, \quad (10)$$

$$P''(k_i z) - k_i^2 P(k_i z) = 0, \quad i = 1, 2, \dots, \quad z = 0, H. \quad (11)$$

The radial profiles of the axial and radial component of mean velocity were measured in two cross sections: immediately under the impeller ($z = z_I$) and above the impeller ($z = z_{II}$). The values of function P and of its derivative P' can be found from the measured radial profiles of components of mean velocity in the following way^{3,5}:

$$F_{ij} = P'(k_i z_j) = \int_0^{D/2} r f_j(r) J_1(k_i r) dr / \int_0^{D/2} r J_1^2(k_i r) dr, \quad (12)$$

$$i = 1, 2, \dots, \quad j = I, II,$$

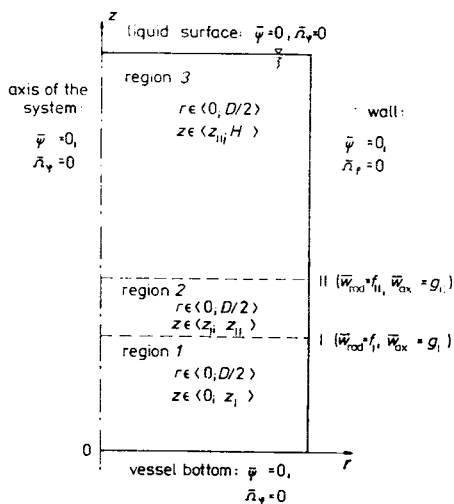


FIG. 2
Boundary conditions in single regions of agitated system

$$G_{ij} = -k_i P(k_i z_j) = \int_0^{D/2} r g_j(r) J_0(k_i r) dr / \int_0^{D/2} r J_0^2(k_i r) dr, \quad (13)$$

$$i = 1, 2, \dots, \quad j = \text{I, II},$$

functions $f_j(r)$ and $g_j(r)$ representing the radial courses (profiles) of the measured components of mean velocity \bar{w}_{rad} and \bar{w}_{ax} in cross sections I and II:

$$f_j(r) = \bar{w}_{rad}(r, z_j), \quad j = \text{I, II}, \quad (14a)$$

$$g_j(r) = \bar{w}_{ax}(r, z_j), \quad j = \text{I, II}. \quad (14b)$$

In this way the boundary conditions were set for upper base of region 1 ($z = z_1$), lower base of region 3 ($z = z_{II}$), and both bases of region 2 ($z = z_I$ and/or $z = z_{II}$) — see Fig. 2, and so the mutual continuity of solution in single regions of system was ensured as it after all corresponds to the physical reality.

Altogether three types of the four inclined blade impellers (see Fig. 3) were investigated: A inclined blade impeller (corresponding to Czechoslovak Standard 691025 (ref.⁷)), B asymmetrically profiled blade impeller⁸, and C strength-profiled blade impeller⁹. For all the given types of impellers, the field of mean velocity and/or mean stream function (see Eq. (3)) was determined, and their properties from the point of view of the flow intensity of agitated charge with respect to the power input were evaluated.

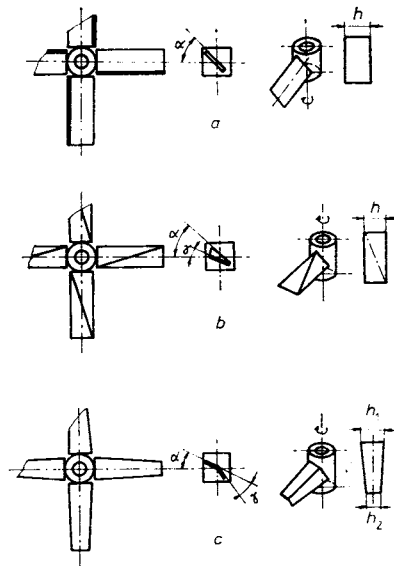


FIG. 3

Investigated types of the four inclined blade impellers: a Plane blade impeller ($\alpha = 25^\circ$, $h = 0.2d$) — type A; b Asymmetrically profiled blade impeller ($\alpha = 30^\circ$, $\gamma = 17^\circ$, $h = 0.2d$) — type B; c Strength-profiled blade impeller ($\alpha = 25^\circ$, $\gamma = 28^\circ$, $h_1 = 0.2d$, $h_2 = 0.12d$) — type C

EXPERIMENTAL

The experiments were carried out in a flat-bottomed cylindrical vessel equipped with four radial baffles (Fig. 1). The vessel placed in a square thermostat was filled with distilled water of temperature $20 \pm 1^\circ\text{C}$, and the experiments took place always under the turbulent regime of flow of agitated charge (the value of the Reynolds number for mixing was always higher than ten thousand). The velocity field in the agitated system was measured by the laser-doppler anemometry of the TSI type^{10,11} with the differential arrangement of the back scatter mode of Ar laser of power 2 W always with three levels of the impeller frequency of revolution. The measurements were carried out in two cross sections immediately under the impeller (cross section I) and in the height of 8 mm above the upper edge of blades of rotating impeller (cross section II). Both the cross sections lay in the plane halving the distance between two adjacent baffles. The impeller always pumped the liquid towards the vessel bottom. In this way the radial profiles (varying coordinate r) were obtained of examined components of mean velocity: axial (\bar{w}_{ax}) and radial (\bar{w}_{rad}).

RESULTS AND DISCUSSION

The results of measurements taken are summarized by continuous curves in Figs 4–6: the radial profiles of axial and radial component of mean velocity for all three compared types of impellers in cross section I under the impeller and in cross section II above the impeller. The found values of components of mean velocity were compared with the impeller tip speed πdn , and so dimensionless quantities

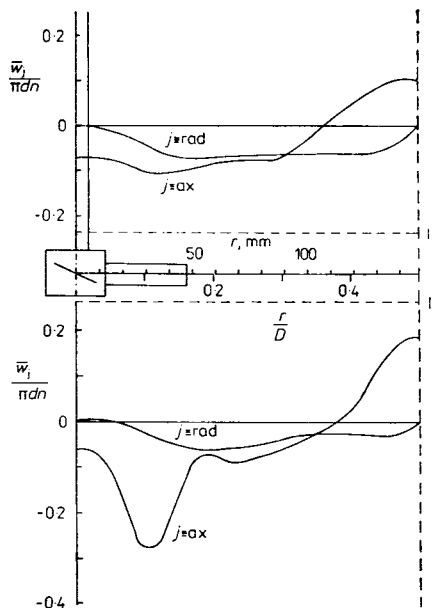


FIG. 4
Radial profiles of dimensionless components of mean velocity under and above the inclined plane blade impeller — type A

were obtained. From the obtained results of experimental investigation of velocity field in the agitated charge under its turbulent flow regime^{12,13} follows that in the chosen place for a given type of impeller, the arbitrary component of mean velocity does not depend on the impeller frequency of revolution. The curves in Figs 4–6 are therefore mean values fitted by the method of centres of gravity through the measured radial profiles always for the given type of impeller in cross sections I and II.

The energy source of charge flow (impeller) considerably influences the velocity field in the impeller vicinity (see Figs 4–6). The profile of axial component of mean velocity $\bar{w}_{ax}/\pi dn$ exhibits a marked maximum under the impeller (cross section I) and a very flat course¹² in the region above the impeller. At the wall, where the direction of flow is opposite (upwards) than in the impeller region, the value of component $\bar{w}_{ax}/\pi dn$ increases practically in a linear way nearly up to the wall itself where the effect of boundary layer only appears by decreasing this velocity component. Of all three impellers investigated, the most marked maximum of quantity $\bar{w}_{ax}/\pi dn$ in the stream at the outlet of region of rotating impeller is shown by the impeller with strength-profiled blades (see Fig. 6) whereas the flattest radial profile

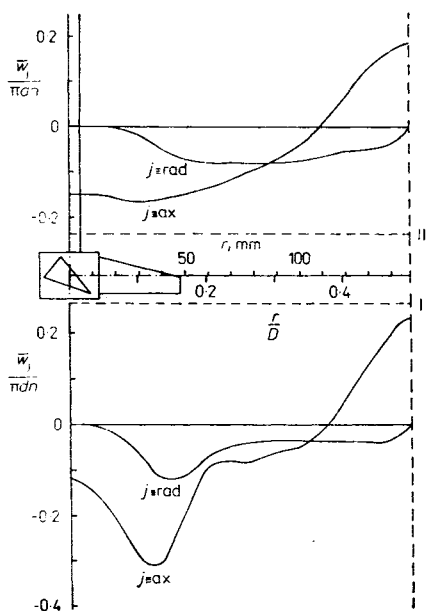


FIG. 5

Radial profiles of dimensionless components of mean velocity under and above the asymmetrically profiled blade impeller — type B

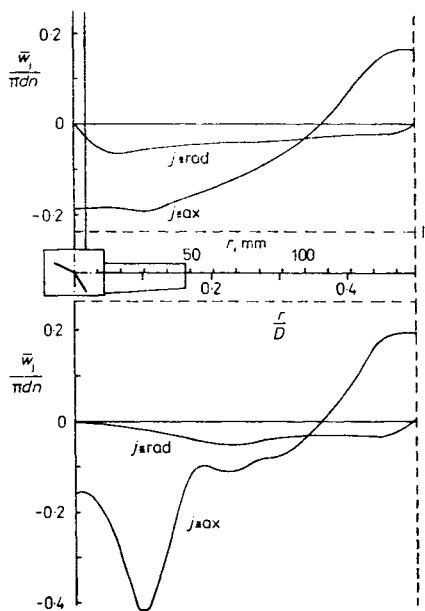


FIG. 6

Radial profiles of dimensionless components of mean velocity under and above the strength-profiled blade impeller — type C

of the given velocity profile is exhibited by the impeller with asymmetrically profiled blades (see Fig. 5). The radial profiles of radial component of mean velocity $\bar{w}_{rad}/\pi dn$ are, unlike the profiles of axial component, considerably flatter and reach also lower values especially in the region under the impeller (cross section 1). This fact confirms the already known results of experiments¹² that the inclined blade impellers may be regarded as impellers producing purely the axial flow.

On using the introduced boundary conditions (see Fig. 2) and Eqs (12)–(14), the courses of the Stokes stream function $\bar{\psi}$ in the systems examined in regions 1, 2, and 3 were determined by solving relation (5) with respect to Eqs (8)–(11); therefore, the measured profiles of the mean velocity components given in Figs 4–6

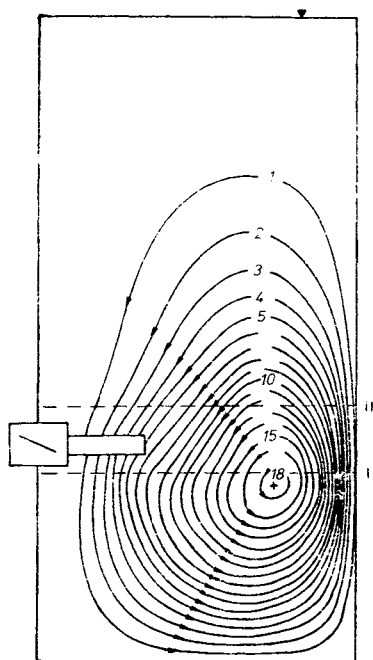


FIG. 7

Streamline field in cylindrical system with radial baffles and flat bottom; the four inclined plane blade impeller — type A ($N = 10$). Number of curve, $\bar{\psi}/nd^3$: 1 0·01; 2 0·02; 3 0·03; 4 0·04; 5 0·05; 6 0·06; 7 0·07; 8 0·08; 9 0·09; 10 0·10; 11 0·11; 12 0·12; 13 0·13; 14 0·14; 15 0·15; 16 0·16; 17 0·17; 18 0·175

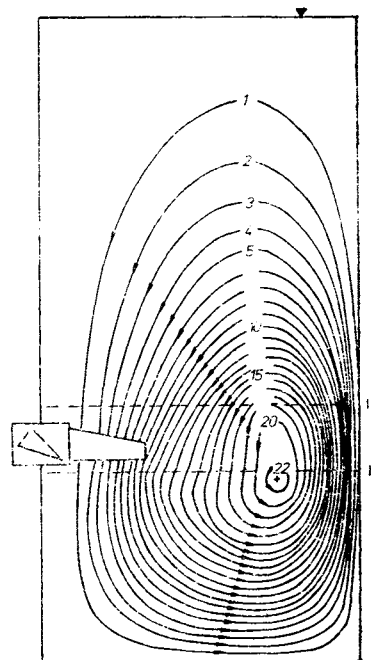


FIG. 8

Streamline field in cylindrical system with radial baffles and flat bottom; the four asymmetrically profiled blade impeller — type B ($N = 10$). Number of curve, $\bar{\psi}/dn^3$: 1 0·01; 2 0·02; 3 0·03; 4 0·04; 5 0·05; 6 0·06; 7 0·07; 8 0·08; 9 0·09; 10 0·10; 11 0·11; 12 0·12; 13 0·13; 14 0·14; 15 0·15; 16 0·16; 17 0·17; 18 0·18; 19 0·19; 20 0·20; 21 0·21; 22 0·212

were exploited, the number of terms in infinite series being reduced to $N = 10$. The calculated courses of the Stokes stream function in dimensionless form ($\bar{\psi}/nd^3$) are plotted in Figs 7–9. The number of terms of the series $N = 10$ was chosen for the selected convergence criterion of the infinite series³ used which required that the changes in the value of dimensionless Stokes stream function should not exceed, on increasing the number of the series terms by one, the value $\Delta(\bar{\psi}/nd^3) = 0.01$ which was considered to be corresponding to the accuracy of determination of the respective components of mean velocity¹³. From the streamline fields constructed (and also the axial and radial components of mean velocity corresponding to them on the basis of validity of relations (3a) and (3b)) follows that the type of impeller used influence considerably the time-averaged circulation pattern of flow of agitated charge under its turbulent regime of flow. Although the basic features of this pattern (e.g., high concentration of streamlines at the vessel wall, nearly pure axial direction of flow from the region of rotating impeller or the position of maximum value of the considered stream function) are nearly identical, the form of streamline field and especially its density in the region above the impeller (above plane II) show significantly different courses in dependence on the type of impeller investigated. The explicitly worst appears to be the inclined plane blade impeller (type A) which brings about high inhomogeneity of streamline field especially at

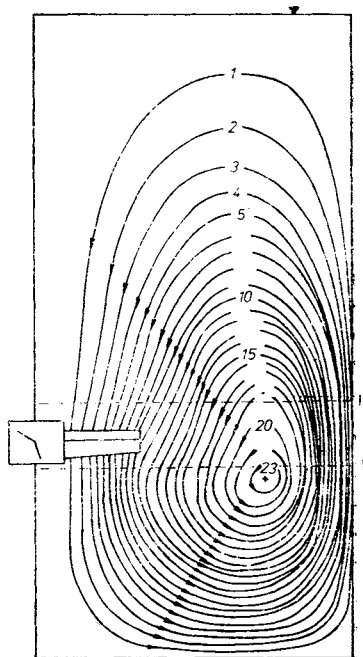


FIG. 9

Streamline field in cylindrical system with radial baffles and flat bottom; the four strength-profiled blade impeller — type C ($N = 10$). Number of curve, $\bar{\psi}/nd^3$: 1 0.01; 2 0.02; 3 0.03; 4 0.04; 5 0.05; 6 0.06; 7 0.07; 8 0.08; 9 0.09; 10 0.10; 11 0.11; 12 0.12; 13 0.13; 14 0.14; 15 0.15; 16 0.16; 17 0.17; 18 0.18; 19 0.19; 20 0.20; 21 0.21; 22 0.22; 23 0.225

the vessel axis and liquid level (see Fig. 7), and on the contrary, the strength-profiled blade impeller (type C) exhibits relatively uniform distribution of the dimensionless Stokes stream function, and consequently also the velocity field in the system even in the region at the liquid level and vessel axis (see Fig. 9). Table I summarizes the basic integral characteristics of the inclined blade impellers (power input criteria of single impellers were considered constant, independent of the Reynolds number).

The respective flow rate criteria \dot{V}_p/nd^3 and \dot{V}_t/nd^3 were calculated on the basis of definition of the Stokes function in an axisymmetrical system, as 2π -multiple of the dimensionless Stokes function value going through the radial coordinate of the impeller radius ($r = d/2$, quantity \dot{V}_p/nd^3) or the maximum value of the dimensionless Stokes function calculated for single arrangements — see legend of Figs 7–9. Values of the power input criteria were found experimentally by the method of turntable¹⁴ using the model equipments identical with those described in the experimental part of this work. It follows from Table I that it is impossible to decide unambiguously between the impeller types B and C which of them is more suitable since the impeller of type C exhibits high values of respective flow rates of charge (and so also of the streamline density and consequently of the velocity field, too), however, with more than double power input. As a complementary evaluating criterion was therefore chosen the impeller energy efficiency

$$E_p \equiv (\dot{V}_p/nd^3)^3 / (P/\rho n^3 d^5), \quad (15a)$$

and/or the total impeller energy efficiency

$$E_t \equiv (\dot{V}_t/nd^3)^3 / (P/\rho n^3 d^5). \quad (15b)$$

TABLE I
Basic hydraulic characteristics of the inclined blade impellers investigated

Type of impeller	\dot{V}_p/nd^3	\dot{V}_t/nd^3	$P/\rho n^3 d^5$	E_p	E_t
A	0.465	1.100	0.510	0.197	2.61
B	0.600	1.332	0.410	0.527	5.76
C	0.678	1.413	0.830	0.376	3.40
D ^a	0.519 ^c	1.081 ^c	0.350 ^d	0.399	3.61
E ^b	0.964 ^c	1.460 ^c	1.70 ^d	0.527	1.83

^a Three blade propeller mixer ($s = d$) according to Czechoslovak Standard 691019a (ref.⁷); ^b six inclined ($\alpha = 45^\circ$) plane blade impeller according to Czechoslovak Standard 691020 (ref.⁷); ^c taken from ref.¹⁷; ^d taken from ref.⁷.

Table I gives as well the values of quantities E_p and E_t calculated for the three blade propeller mixer ($s = d$) according to Czechoslovak Standard 691019a (ref.⁷) (impeller D) and for the six blade impeller with inclined blades at the angle $\alpha = 45^\circ$ ($h = 0.2d$) according to Czechoslovak Standard 691020 (ref.⁷) (impeller E) from the data of cited literature^{7,17}. From the values of calculated energy efficiencies of these impellers follows that both of them reach high values of quantity E_p but the value of quantity E_t for the impeller of type E is practically the lowest for the impeller types compared. The six inclined blade impeller is therefore suitable to be employed for those operations in which is decisive the impeller pumping effect \dot{V}_p and not the total flow rate of agitated charge \dot{V}_t (e.g., for suspending the solid particles in liquid). The three blade propeller mixer ($s = d$) lies with its energy efficiency between the compared types of impellers B and C. However, it is more difficult to manufacture than the above-mentioned types of blade impellers and therefore also more expensive.

The given quantities are, under the turbulent flow regime of agitated charge, directly proportional⁸ to the impeller hydraulic efficiency and characterize therefore the impeller efficiency to transfer the supplied power input to the impeller circulation effects, i.e., its ability to bring about the as large as possible convective flow. From this point of view, the type of impeller B (the impeller with asymmetrically profiled blades) appears to be explicitly the most convenient and can replace by its shape the more difficult to manufacture impellers with airfoil profiles of blade shapes^{1,2}, e.g., the impeller of type D. The advantage of impeller of type C (the strength-profiled blade impeller) is then the possibility of its use at higher impeller tip speeds when the elimination or design simplification of the gear box between the driving device (motor) and the impeller contributes to reducing the investment costs of designing the plant technological equipment or even increases the mechanical efficiency of the gear box used and therefore also the utilization of energy to the technological process itself. In conclusion of this study it is still suitable to remark that the approximate two-dimensional procedure is concerned which holds for fully developed turbulent flow of agitated charge. The study of circulation of mechanically agitated liquid under the laminar regime of flow of agitated charge^{15,16} leads to a more exact (three-dimensional) description of its flow. However, this procedure could not be used in the submitted study since the used choice of boundary conditions and the simplification (neglecting) of the respective class of viscous forces seems hitherto to be the only viable method of solution of the phenomenologically more complex turbulent flow of agitated charge in the mathematical analytical way.

LIST OF SYMBOLS

B	integration constant, $m^2 s^{-1}$
b	radial baffle width, m
C	integration constant, $m^2 s^{-1}$

D	integration constant, $m^2 s^{-1}$
D	vessel diameter, m
d	impeller diameter, m
E	integration constant, $m^2 s^{-1}$
E_p	impeller energy efficiency, Eq. (15a)
E_t	total impeller energy efficiency, Eq. (15b)
F	function defined by Eq. (12), $m s^{-1}$
f_j	radial component of mean velocity in j-th cross section, $m s^{-1}$
G	function defined by Eq. (13), $m s^{-1}$
g_j	axial component of mean velocity, $m s^{-1}$
H	height of liquid level at rest in vessel above bottom, m
H_2	height of lower edge of impeller blade above bottom, m
h	impeller blade width, m
J_ν	cylindrical (Bessel) function of first kind of index ν
k	characteristic number, m^{-1}
N	number of terms of series for considered solution of flow equation
n	frequency of impeller revolution, s^{-1}
P	hyperbolic function defined by Eq. (8), $m^2 s^{-1}$
P	impeller power input, W
$P/\rho n^3 d^5$	power input criterion (power number)
r	radial coordinate, m
s	pitch of propeller mixer, m
\dot{V}_p	pumping efficiency of impeller, $m^3 s^{-1}$
\dot{V}_p/nd^3	flow rate criterion
\dot{V}_t	total flow rate of agitated charge, $m^3 s^{-1}$
\dot{V}_t/nd^3	total flow rate criterion
w	velocity of agitated charge, $m s^{-1}$
z	axial coordinate, m
α	angle of impeller blade inclination, $^\circ$
γ	angle of impeller blade inclination, $^\circ$
λ	root of function J_1
Ω	vorticity, s^{-1}
ρ	density of agitated charge, $kg m^{-3}$
$\bar{\psi}$	Stokes stream function, $m^3 s^{-1}$
$\bar{\psi}/nd^3$	dimensionless Stokes stream function

Subscripts and Superscripts

ax	axial
i	summation index
j	summation index
rad	radial
ϕ	tangential
o	initial value of axial coordinate in given region
l	final value of axial coordinate in given region
I	cross section of velocity measurement under impeller
II	cross section of velocity measurement above impeller
—	time-averaged quantity

REFERENCES

1. Oldshue J. Y.: *Proc. 5th Europ. Conference on Mixing*, p. 195. Würzburg 1985.
2. Weetman R. J., Oldshue J. Y.: *Proc. 6th Europ. Conference on Mixing*, p. 43. Pavia 1988.
3. Hošťálek M., Fořt I.: *Collect. Czech. Chem. Commun.* 50, 930 (1985).
4. Hošťálek M., Fořt I.: *Collect. Czech. Chem. Commun.* 50, 2396 (1985).
5. Fořt I., Hošťálek M., Laufhütte H. D., Mersmann A. B.: *Collect. Czech. Chem. Commun.* 52, 1416 (1987).
6. Hošťálek M., Fořt I.: *Collect. Czech. Chem. Commun.* 52, 1888 (1987).
7. Czechoslovak Standard 6910. VÚCHZ — CHEPOS, Brno 1969.
8. Fořt I., Medek J.: *Proc. 6th Europ. Conference on Mixing*, p. 51. Pavia 1988.
9. Seichter P., Vítek O., Jaroměřský J., Khol M.: *Czech.* 248—314, 1984.
10. *Technical Proposal of LDV System for Turbomachinery*. TSI Inc., St. Paul 1981.
11. Klaboch L., Ptáčník M., Lamka J., Fořt I.: *Proc. 6th Europ. Conference on Mixing*, p. 56. Pavia 1988.
12. Fořt I. in: *Mixing. Theory and Practice*, Vol. III. (V. W. Uhl and J. B. Gray, Eds). Academic Press, New York 1986.
13. Fořt I., Klaboch L., Ptáčník M., Lamka J., Medek J.: Unpublished results.
14. Uhl V. W., Gray J. B.: *Mixing. Theory and Practice*, Vol. I. Academic Press, New York 1966.
15. Bertrand J., Couderc J. P.: *Can. J. Chem. Eng.* 60, 738 (1982).
16. Hiraoka S., Yamada I., Aragaki T., Nishiki H., Sato A., Takagi T.: *J. Chem. Eng. Jpn.* 21, 79 (1988).
17. Fořt I., Valešová H., Kudrna V.: *Collect. Czech. Chem. Commun.* 36, 164 (1971).

Translated by J. Linck.